A Comparative Study of Refractive Index Sensors Based on Bare TFBG and SPR-TFBG

Jiang Qi　Hu Debo

(*School of Control Science and Engineering*, *Shandong University*, *Jinan*, *Shandong* 250061, *China*)

Abstract　The refractive index sensing principle of tilted fiber Bragg grating (TFBG) and tilted fiber Bragg grating with surface plasmon resonance (SPR-TFBG) is provided. The transmission spectrum and reflection spectrum of TFBG with 8° tilt angle and 1550 nm central wavelength are given. After that, refractive index sensing experiments are carried out using bare and gold deposited TFBG, respectively. The results prove that the deposited gold layer improves the refractive index sensitivity dramatically.

Key words　fiber optics; tilted fiber Bragg grating; surface plasmon resonance; refractive index

中图分类号　TP212.14　　**文献标识码**　A　　**doi**: 10.3788/LOP49.080602

基于倾斜光纤光栅及其表面等离子效应的折射率传感比较研究

蒋　奇　胡德波

(山东大学控制科学与工程学院, 山东 济南 250061)

摘要　介绍了倾斜光纤光栅作为折射率传感器的测量原理,给出它的倾斜角8°与中心波长1550 nm的反射谱与透射谱,分析了具有表面等离子的倾斜光纤光栅传感机理。为验证折射率传感的可能性与优点,进行了蔗糖浓度溶液的裸倾斜光纤光栅与镀金的倾斜光纤光栅的折射率测量分析,证明镀金后的表面等离子效应倾斜光纤光栅折射率传感器其灵敏度大大增加。

关键词　光纤光学;倾斜光纤光栅;表面等离子共振;折射率

OCIS codes　060.2370; 240.6680

1　Introduction

Tilted fiber Bragg grating (TFBG) and uniform fiber Bragg grating (FBG) both belong to the short period fiber grating of which the grating period is several hundreds of nanometers[1~3]. The difference between them is that the grating plane of the TFBG is not parallel to the cross section of the fiber but tilted by an angle.

The structure difference between TFBG and FBG leads to the distinct differences of their spectra. Only the Bragg resonance peak can be observed in the reflection spectrum of FBG[4,5]. However, the tilted grating planes could couple the incident light to a contra-propagating core mode as well as a series of contra-propagating cladding modes distributed at discrete wavelengths below the Bragg wavelength[6]. A peak which represents the core mode can be observed in the reflection spectrum; correspondingly, a notch will present itself in the transmission spectrum. The contra-propagating cladding modes attenuate rapidly and are therefore not observable in the reflection spectrum but observed as numerous discrete notches in the transmission spectrum. Specifically, several low order cladding modes would fold up to form a strong ghost mode[7]. TFBG has been studied as refractive index sensor, strain sensor with temperature compensation, micro-bend sensor, vibration sensor and so on in recent years[4~7]. The constructed refractive index sensor by TFBG with surface plasmen resonance (SPR) has also been put forward by Carleton University researching group[5].

收稿日期: 2012-03-17; **收到修改稿日期**: 2012-05-02; **网络出版日期**: 2012-06-07

基金项目: 教育部新世纪优秀人才培养计划(NCET-10-0541)、国家自然科学基金(51079080)和山东大学自主创新基金(2012ZD015)资助课题。

作者简介: 蒋　奇(1973—),男,教授,主要从事检测技术、光纤传感器方面的研究。E-mail: jianqi@sdu.edu.cn

In this paper, we carry out a comparative study of refractive sensors based on bare TFBG and SPR-TFBG. Experimental results show that gold deposited SPR-TFBG has a significantly improved sensitivity for refractive index measurement.

2 Sensing principle

The schematic of a TFBG is shown in Fig. 1. The grating plane is tilted by an angle θ to the cross section of the fiaer core.

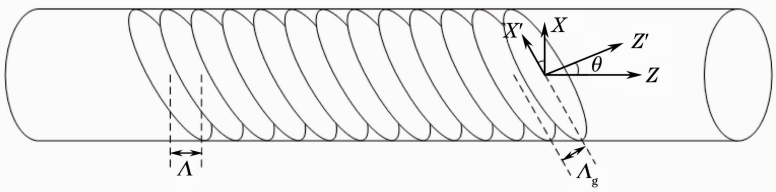

Fig. 1 TFBG with a tilt angle θ in the core of SMF

The reflection and transmission spectra of TFBG with tilted angle of 8° at the 1550 nm central wavelength are shown in Fig. 2.

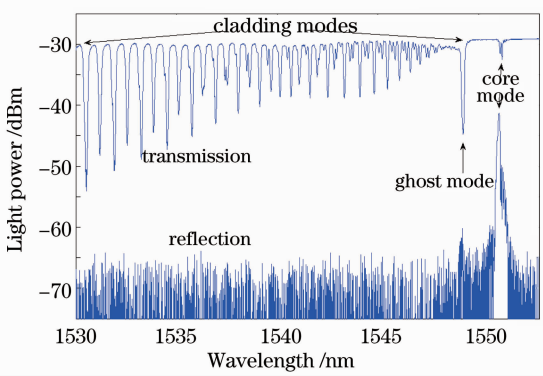

Fig. 2 Transmission and reflection spectra of TFBG

The wavelength of the ith order cladding mode of TFBG can be expressed as [7]

$$\lambda^{i}_{\text{clad}} = (n^{i}_{\text{eff,core}} + n^{i}_{\text{eff,clad}})\Lambda/\cos\theta, \tag{1}$$

where $n^{i}_{\text{eff,core}}$ and $n^{i}_{\text{eff,clad}}$ represent the effective refractive indices of the fiber core and cladding for the ith order cladding mode, respectively.

Because the cladding modes propagate in the cladding of TFBG of which the effective refractive index is influenced by the surrounding refractive index (SRI), it can be predicted that the wavelength of cladding modes will shift with the SRI. The expected wavelength can be expressed as

$$\Delta\lambda^{i}_{\text{clad,SRI}} = \left[\frac{\Lambda}{\cos\theta}\frac{\partial(n^{i}_{\text{eff,core}} + n^{i}_{\text{eff,clad}})}{\partial n_{\text{SRI}}} + \frac{n^{i}_{\text{eff,core}} + n^{i}_{\text{eff,clad}}}{\cos\theta}\frac{\partial\Lambda}{\partial n_{\text{SRI}}}\right]\Delta n_{\text{SRI}}, \tag{2}$$

where Δn_{SRI} is the variation of SRI. The effective refractive index of the fiber core and the grating period will not change as the SRI changes, thus, $\partial n^{i}_{\text{eff,core}}/\partial n_{\text{SRI}} = 0$, $\partial\Lambda/\partial n_{\text{SRI}} = 0$. Equation (2) can be simplified to

$$\Delta\lambda^{i}_{\text{clad,SRI}} = \frac{\Lambda}{\cos\theta}\frac{\partial n^{i}_{\text{eff,clad}}}{\partial n_{\text{SRI}}}\Delta n_{\text{SRI}}. \tag{3}$$

Total internal reflection (TIR) of the cladding modes can be achieved at the interface between the cladding of TFBG and the surrounding material, so it is convenient to exploit TFBG to construct a SPR refractive index sensor by depositing a layer of gold at the surface of the bare TFBG. As the incident light propagates in the TFBG, a part of the light will be coupled to the cladding to form the cladding modes. These cladding modes hit the interface between the cladding and the metal film at different angles and stimulate the surface plasmon wave (SPW) at the exterior surface of the metal film. As a result of SPW, a SPR peak will present itself in the transmission spectrum of TFBG-SPR. When the refractive index of the SRI changes, the wavelength of the resonance peak will shift.

3 Experiments and results

3.1 Optical circuit of experiments

The experimental optical setup is demonstrated in Fig. 3. The bare TFBG and SPR-TFBG would be placed in the sample tank respectively. Here, SPR-TFBG was fabricated with 50 nm gold coating in a very simple vacuum sputtering deposition system. The used optical source was C + L band amplified spontaneous emission (ASE) broadband light source (BBS) of which the spectrum ranges from 1525 to 1610 nm. The used optical spectrum analyzer (OSA) was AQ6317B.

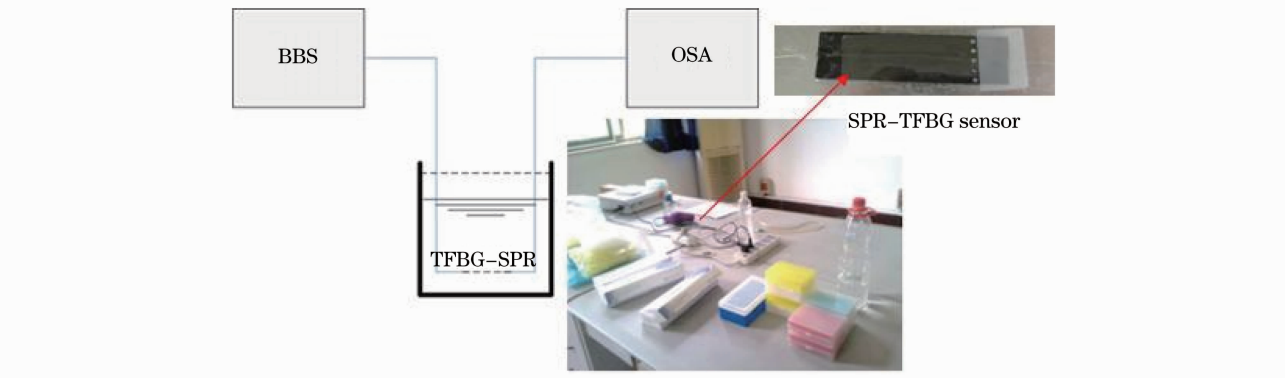

Fig.3 Experimental optical circuit and picture

3.2 Process of experiments

A group of sucrose solution with different concentrations was prepared for the refractive index sensing experiment. The mass concentrations of the solutions were 11.1%, 20.0%, 27.3%, 33.3% and 38.5%, respectively. According to Ref.[6], the refractive indices of the solutions can be calculated as shown in Table 1. Meanwhile, the refractive indices of different solutions were tested via WYA-Z Abbe refractometer. The sucrose solutions with different concentrations were added to the sample tank successively in an ascending order to keep in close touch with the surface of the bare TFBG or SPR-TFBG[7,8], and then the spectra were saved to be used as raw data. The bare TFBG or the SPR-TFBG and the sample tank must be cleaned thoroughly before the solution is added to the tank. The room temperature and the temperature of the solutions must be constant during the experiment process.

Table 1 Relation between solution concentration and refractive index

Mass concentration (20 ℃) / %	Refractive index (20 ℃, 589 nm)
0	1.333
11.1	1.350
20.0	1.364
27.3	1.376
33.3	1.387
38.5	1.397

3.3 Experiment result of bare TFBG

Figure 4 demonstrates the spectrum evolution of a cladding mode at the wavelength 1530 nm of the bare TFBG as the surrounding refractive index varies from 1.333 to 1.397. It is obvious that the central wavelength of the cladding mode shifts to the long wavelength direction as the surrounding refractive index increases.

Figure 5 is a quantitative description of the relation between the central wavelength of the cladding mode and the refractive index of the sucrose solution, which shows that the bare TFBG is sensitive to the solution refractive index with a relatively low sensitivity of 2.16 nm/RIU (RIU means refractive index unit).

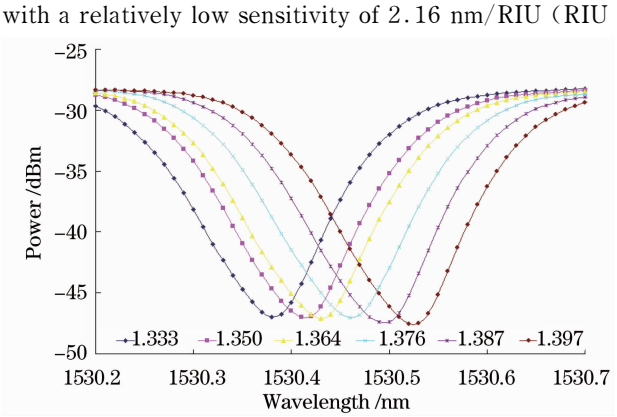

Fig.4 Spectrum evolution of cladding mode of TFBG with different surrounding refractive indices

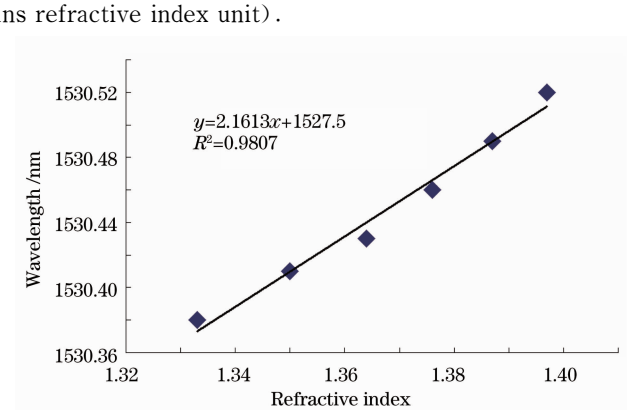

Fig.5 Relation between cladding mode wavelength and solution refractive index

3.4 Experiment result of SPR-TFBG

Figure 6 demonstrates the spectrum evolution of the SPR-TFBG as the surrounding refractive index varies from 1.333 to 1.397. It is obvious that the SPR wavelength of the SPR-TFBG sensor shifts to the long wavelength direction as the surrounding refractive index increases.

Figure 7 is a quantitative description of the relation between the SPR wavelength of the SPR-TFBG sensor and the refractive index of the sucrose solution, which shows that the SPR-TFBG sensor is very sensitive to the solution refractive index with a much higher sensitivity of 698.77 nm/RIU than that of the bare TFBG.

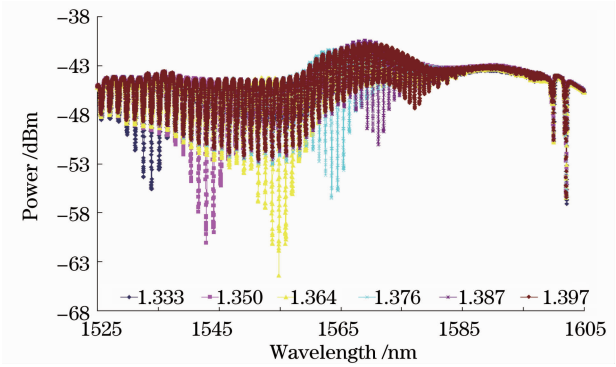

Fig. 6 Spectrum evolution of SPR-TFBG with different surrounding refractive indices

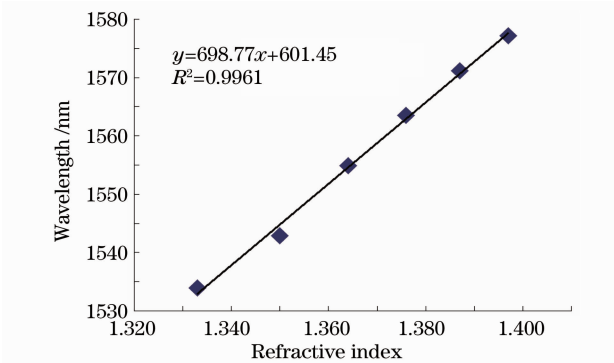

Fig. 7 Relation between SPR wavelength and solution refractive index

4 Conclusion

Refractive index sensing experiments were conducted to compare the sensing characteristics of the bare and gold deposited TFBGs[9,10]. The results show that the gold deposited TFBG possesses much higher sensitivity than the bare one. The sensitivity of the gold deposited TFBG can be up to 698.77 nm/RIU, which is 323 times larger than that of the bare TFBG.

Acknowledgements

The authors would like to acknowledge the research team of Prof. J. Albert of Carleton University for their support.

References

1 Wu Fei, Zhao Jing, Liu Bin *et al*.. Study on local temperature characteristics of fiber Bragg gratings[J]. *Optoelectronics Letters*, 2010, **6**(2): 98～102

2 Yuan Yinquan, Liang Lei, Zhang Dongsheng. Spectra of fiber Bragg grating and long period fiber grating undergoing linear and quadratic strain[J]. *Optoelectronics Letters*, 2009, **5**(3): 182～185

3 S. Grice, W. Zhang, K. Sugden *et al*.. Liquid level sensor utilising a long period fiber grating[C]. *SPIE*, 2009, **7212**: 72120C

4 G. Laffont, P. Ferdinand. Tilted short-period fibre-Bragg-grating-induced coupling to cladding modes for accurate refractometry[J]. *Meas. Sci. Technol.*, 2001, **12**(7): 765～770

5 C. Chen, L. Xiong, C. Caucheteur *et al*.. Differential strain sensitivity of higher order cladding modes in weakly tilted fibre Bragg gratings[C]. *SPIE*, 2006, **6379**: 63790E

6 K. S. Lee, T. Erdogan. Fiber mode coupling in transmissive and reflective tilted fiber gratings[J]. *Appl. Opt.*, 2000, **39**(9): 1394～1404

7 E. Chehura, S. W. James, R. P. Tatam. Temperature and strain discrimination using a single tilted fibre Bragg grating[J]. *Opt. Commun.*, 2007, **275**(2): 344～347

8 F. Abdelmalek. Surface plasmon resonance based on Bragg gratings to test the durability of Au-Al films[J]. *Mater. Lett.*, 2002, **57**(1): 213～218

9 G. Nemova, R. Kashyap. Modeling of plasmon-polariton refractive-index hollow core fiber sensors assisted by a fiber Bragg grating[J]. *J. Lightwave Technol.*, 2006, **24**(10): 3789～3796

10 T. Allsop, R. Neal, S. Rehman *et al*.. Generation of infrared surface plasmon resonances with high refractive index sensitivity utilizing tilted fiber Bragg gratings[J]. *Appl. Opt.*, 2007, **46**(22): 5456～5460